THE JOURNAL OF PHYSICAL CHEMISTRY B

Article

pubs.acs.org/JPCB

A Real Time Analysis of the Self-Assembly Process Using Thermal Analysis Inside the Differential Scanning Calorimeter Instrument

Debmalya Roy,* Babita Shastri, and K. Mukhopadhyay

Nanoscience and Technology Division, DMSRDE, GT Road, Kanpur, India-208013

Supporting Information

ABSTRACT: The supramolecular assembly of the regioregular poly-3-hexylthiophene (rr-P3HT) in solution has been investigated thoroughly in the past. In the current study, our focus is on the enthalpy of nanofiber formation using thermal analysis techniques by performing the self-assembly process inside the differential scanning calorimetry (DSC) instrument. Thermogravimetric analysis (TGA) was carried out to check the concentration of the solvent during the self-assembly process of P3HT in *p*-xylene. Ultraviolet visible (UV−vis) spectophotometric technique, small-angle X-ray scattering (SAXS) experiment, atomic force microscopic (AFM), and scanning electron microscopic (SEM) images were used to characterize the different experimental yields generated by cooling the reaction mixture at desired temperatures. Comparison of the morphologies of self-assembled products at different fiber formation temperatures gives us an idea about the possible crystallization parameters which could affect the P3HT nanofiber morphology.

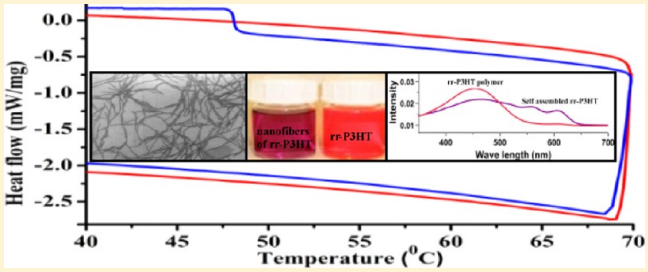

INTRODUCTION

The self-assembly of the organic semiconducting polymer into the nanostructure with novel morphology and property has attracted an increasing interest as a new approach for materials science, chemical synthesis, and nanofabrication.[1−3] Among various semiconducting polymers, regioregular poly-3-hexylthiophene (rr-P3HT) is widely studied due to its superior optoelectonic property and chemical stability. The rigid thiophene backbone with a regular head-to-tail arrangement of pendant hexyl side chains allows constructing an efficient π to π stacking of the nanocrystalline lamellae.[4−6] The transportation of electrons in the crystalline portion occurs mainly through the intrachain and interchain transport mechanism, whereas in the amorphous portion the same is proceeding through the hopping or tunnelling process.[7] The ordering of P3HT thin film thus leads to the enhancement of the charge carrier mobility in the thin-film transistor by several orders of magnitude.[8] The order and disorder phases in P3HT were explained as microcrystallite and amorphous phase, respectively.[9] Nanofibers of polythiophene derivatives have been prepared by various procedures like the template method,[10] electrospinning,[11] nontemplate method,[12] Langmuir−Blodgett method,[13] dip-pen nanolithography,[14] copolymerization,[15] molecular combing,[16] self-organization on a substrate during drying,[17] and self-organized hierarchical whisker formation in solution.[18]

The order−disorder transformation for whisker formation has been investigated thoroughly due to the low cost and mass production of nanofibers.[19−21] The self-assembled morphology of rr-P3HT showed potential application as the donor material for organic photovoltaics (OPV) compared to its pristine structure.[22−24] rr-P3HT, which has been extensively used as donor material, could not absorb photons above the 1.9 eV energy and hence does not harvest more photons from the solar spectrum.[25] Another major bottleneck of the P3HT-based OPV system is the longer device annealing time at a high temperature to make the polymer film more crystalline and compact. Device annealing generally alters the physical and chemical properties of the film, which results in lower stability and performance of OPV devices.[26] The use of rr-P3HT nanofibers as donor material for the fabrication of high-performance OPV has a three-fold advantage. The much longer conjugation length in the fiber structure red-shifts the absorption to the near-IR region. It has been reported that 52% of the energy in the air−mass 1.5 global (AM 1.5G) solar irradiance spectrum is from the NIR region and the higher absorption of rr-P3HT nanofibers in this region helps to harvest more photons from sunlight.[22,27] The second advantage of using nanofibers of rr-P3HT as donor material in OPV is the much higher packing density. The more compact orientation of polymer microstructures is possible due to the nanosized diameters of the fiber structures. The higher number of oriented light absorbing chromophores thus could be accommodated in the active area of the OPV device by using fiber type polymer microstructure.[28] The third and most important advantage of the use of nanofibers of rr-P3HT as electron donor is to avoid the device annealing step at high temperature for the long duration. The nanofibers of rr-P3HT

Received: November 27, 2011
Revised: June 9, 2012
Published: June 12, 2012

   dx.doi.org/10.1021/jp211408e | *J. Phys. Chem. B* 2012, 116, 7920−7925

are capable of constructing a highly crystalline film without annealing and hence drastically enhance the stability and performance of OPVs.[29]

The higher molecular weight fraction of rr-P3HT in a solvent, in which the sample shows the strong temperature dependent solubility, generally tends to transform from flexible coils to rigid-rod by slowly cooling the temperature.[30,31] At high temperature rr-P3HT is soluble in *p*-xylene or cyclohexanone due to the free rotation of alkyl side chains. However, upon decreasing the solubility by slowly lowering the temperature of the solution, P3HT rods self-assembled in a face-to-face fashion where the hexyl side chains are organized in a planar, zigzag, or tilting fashion.[18−21] The more ordered rod has the lower internal energy; however, the more disordered coil has greater entropy.[32] To avoid the unfavorable interaction between the poorly soluble backbone and hydrocarbon solvent, rr-P3HT undergoes conformational transition from random twisted to a more planar and ordered state. 1D aggregation of rr-P3HT could be triggered when the polarity of the chlorobenzene or *o*-dichorobenzene solution is decreased by the addition of nitrobenzene or hexane.[33,34]

The conformational transformation of rr-P3HT in solution for whisker formations either by lowering the temperature of the solvent or by adding poor solvent to promote the fraction of microcrystals is well documented in the literature.[4−7,18−21,32−34] It is also well understood that the order−disorder transformation in solution state is mainly govern by the regioregularity of P3HT and the concentration of the solution. The solution having a P3HT concentration higher than 2 wt % leads to the formation of a stable gel at lower temperature. However, the fiber type morphology entrapped in the gel has also been reported in the literature.[19,35] By disturbing the chain regularity of P3HT, the crystallinity of the polymer matrix could be significantly reduced, which renders the self-organization of the polymer chain into a well-ordered lamellar sheet. Regio-random P3HT does not orient to a well-order aggregation in solution; however, a single-chain conformational change has been reported. In the solid state the non-regio-regular P3HT films were shown to adopt more ordered orientations depending on the structures of the thin films which are influenced by the film casting conditions.[36−38]

In this study, our focus is to detect any difference in heat loss during crystallization of P3HT from solution by differential scanning calorimetry (DSC) technique. Above the glass transition temperature, the crystalline polymers generally gained enough energy to move into very ordered arrangements by giving off heat that one can measure by exothermic transition in DSC. Here our system is different and the crystallization of P3HT is occurring in solution. The heat flow sensitivity scale in a modern DSC instrument is now in the range of microwatts and nanowatts region,[39] so a small heat loss during crystallization in the solution should easily be identified. We have therefore carried out the self-assembly process of P3HT in *p*-xylene on a perforated aluminum hermetic pan placed inside the DSC instrument at inert atmosphere. Thermogravimetric analysis (TGA) was performed for detection of the change in concentration of the solvent during the self-assembly process. Comparison of the morphology of self-assembled products at different fiber formation temperatures by isothermal heating along with the isochronal heating in DSC instrument gives us an idea about the crystallization parameters which govern the morphology of the nanofibers of P3HT. The parallel experimentations on different concentrations, cooling rates, reaction times, and non-regio-regular P3HT were used as supporting data which corroborate well with the self-assembled results of P3HT in the literature.[4−7,18−21,32−34]

EXPERIMENTAL SECTION

Electronic grade rr-P3HT and spectroscopic grade *p*-xylene were purchased from Sigma-Aldrich Chemical. The higher weight fraction of rr-P3HT was isolated by the solvent fractionation method for the crystallization experiments by using the standard procedure.[40] The higher weight fraction of the rr-P3HT is referred to as rr-P3HT(h) in the text. To check the rate of evaporation of the 0.01 wt % solution of rr-P3HT(h) dissolved in *p*-xylene, thermogravimetric experiment was carried out on a Mettler Toledo TGA/SDTA 851^e thermogravimetric analyzer from 20 to 160 °C at a 10 deg/min heating rate and 50 mL/min nitrogen flow. The in situ nanofiber formation was carried out inside a differential scanning calorimeter DSC Q200 V24.4 Build 116. One milligram of rr-P3HT(h) was dissolved in 1.1 g of *p*-xylene that was preheated at 70 °C and the solution was then allowed to cool rapidly at the inert atmosphere. A 7.8 mg sample of this solution was transferred on a perforated aluminum hermetic pan and placed inside the DSC instrument, which was kept in an inert atmosphere at 50 mL/min nitrogen flow rate. DSC experiments were performed in the temperature range of −10 to 70 °C at the 10 deg/min heating rate and at different cooling rates. For self-assembly at the desired temperature, the solution placed in the hermetic pan at inert atmosphere was heated at 70 °C by 10 deg/min and then the solution was cooled at 0.5 deg/min to the desired self-assembly temperature by the isochronal manner. Isothermal heating was then performed at that temperature for the desired duration and then the solution was rapidly cooled isochronally at 30 deg/min to room temperature. The perforated aluminum pan was taken out after the experiment, then content was dispersed into 5 mL of *p*-xylene by vigorous shaking and characterized subsequently by ultraviolet−visible (UV−vis) spectroscopic, atomic force microscopy (AFM), and scanning electron microscopic (SEM) studies.

For comparison, another set of nanofiber formations by self-assembly were carried out outside the DSC instrument by the reported procedure[19] and then the products were characterized. In brief, rr-P3HT(h) of 0.01 wt % in *p*-xylene was taken into a two-necked round-bottomed flask equipped with a condenser and a gas inlet. The solution was heated to 70 °C and then slowly cooled (30 deg/h) to 45 and 35 °C in inert atmosphere and in the absence of light. The solutions were kept undisturbed in inert atmosphere at the dark for 08 and 24 h in the corresponding temperatures of 45 and 35 °C. A small fraction of the products were taken after 08 and 24 h and the characterizations were carried out. UV−vis absorption was recorded on a Jasco V-630 double beam UV−vis spectrophotometer in spectroscopic grade *p*-xylene as solvent, using *p*-xylene as the standard reference. For AFM and SEM studies, the silicon substrates were cleaned by soap solution first followed by deionized water and acetone and then dried in a vacuum oven overnight. The cleaned silicon wafers were preheated at 45 and 35 °C and the nanofiber solutions were drop casted on the corresponding preheated silicon wafers, respectively. AFM images were taken on an AFM Nanoscope II, Digital Instruments Inc., USA and SEM images were taken on a SUPRA 40 VP, Gemini, Carl Zeiss, Oberkochen,

dx.doi.org/10.1021/jp211408e | J. Phys. Chem. B 2012, 116, 7920−7925

Germany. Small-angle X-ray scattering (SAXS) experiments were carried out by using the powder samples of the self-assembled products obtained from two different temperatures of 45 and 35 °C, respectively. To obtain the self-assembled product in powder form, the individual solutions were quickly transferred into the pyrex centrifuge tube preheated at the desired temperature with a Teflon cap, which were then placed in the Remi Elektrotechnik Ltd., Microprocessor Research Compufuge, PR-24 ultra centrifuge. The solution was then ultracentrifuged at 5000 rpm for 30 min. The nanofibers were stuck onto the tube walls and the yellow *p*-xylene was settled to the bottom of a centrifuge tube as supernatant liquid. *p*-Xylene was decanted out of the centrifuge tube and fresh *p*-xylene was again added and centrifuged. This process was repeated unless the supernatant liquid became colorless.

RESULTS AND DISCUSSION

The rate of evaporation of *p*-xylene from the 0.01 wt % solution of rr-P3HT(h) was measured by using TGA at inert atmosphere and it was found that 10% *p*-xylene was evaporated while the temperature reached 70 °C (Supporting Information). For the in situ nanofiber formation, 10% extra *p*-xylene was used to make a 0.01 wt % solution of rr-P3HT(h). The DSC thermogram of the 0.01 wt % solution of rr-P3HT(h) in *p*-xylene showed the melting and freezing peaks for the solvent (Figure 1). In a typical self-assembly process of rr-P3HT in

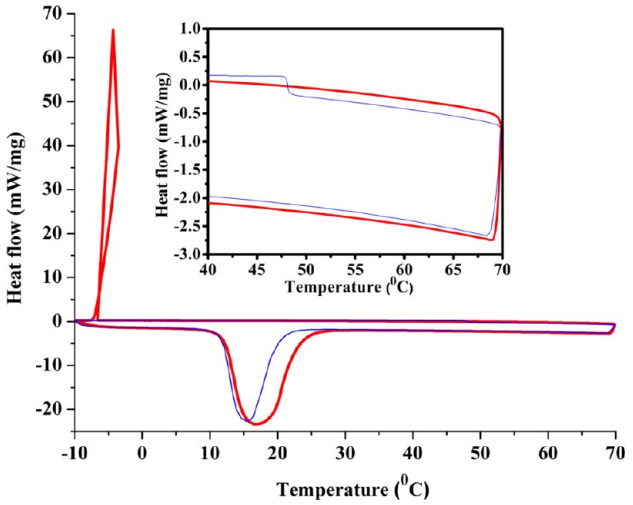

Figure 1. DSC thermogram of 0.01 wt % solution of rr-P3HT(h) dissolved in *p*-xylene from −10 to 70 °C at a 10 deg/min heating rate and 1 deg/min cooling rate with 50 mL/min nitrogen flow indicating first heating and cooling by the red thick line and the second heating and cooling by the blue thin line. In the inset the heating and cooling curves were expanded to show the shift in the rate of heat flow.

solution, the flexible side chains take an ordered geometry to minimize the intra- and intermolecular interactions and produce a perfectly relaxed polymer macrostructure. The driving force in crystallization of P3HT by the orientation of the alkyl side chains in solution is the reduction in total internal energy due to the energy-minimized morphology of the whole system.[17] To check if the crystallization process of P3HT in solution is affected by the heat energy released by the solvent during cooling, we carried out the self-assembly process of the rr-P3HT(h) in *p*-xylene inside the DSC instrument at different cooling rates and at different crystallization temperatures. The cooling curve of the DSC (Figure 1) does not indicate any absorption of the heat energy for crystallization by the self-assembly of rr-P3HT(h) unlike the solid state phase transitions of P3HT, which was studied with use of similar experimental techniques earlier.[41] The second heating on the sample was carried out to examine that the sufficient *p*-xylene was still there for the self-assembly of rr-P3HT(h) (Figure 1). However it was found that most of the *p*-xylene was evaporated out during the course of second heating to 70 °C and hence there was a shift in the rate of heat flow at the second cooling (Figure 1) for the switching over the phase from liquid to solid.

Self-assembly of rr-P3HT(h) inside the DSC instrument failed to produce any evidence of the use of heat energy from the solution for the crystallization of the P3HT in solution. It is thus the decrease of solubility of P3HT in the solution during cooling that is responsible for the crystallization of P3HT in solution. The formation of nanofibers by self-assembly therefore depends on the quality of the crystal formation, which corroborates with the fact that slow cooling produces nanofibers whereas fast cooling does not precipitate any self-assembled product.[17−19] The production of nanofibers of P3HT occurs by cooling only in *p*-xylene[1,17−19] or cyclohexanone[17] or anisole;[42] however, the formation of P3HT fibers in any solvent by adding nonpolar solvent[33,34] confirms our finding in DSC experimentation that it is the decreasing solubility of the solvent that leads to the crystallization by self-assembly in solution.

To obtain the fiber morphology inside the DSC instrument, the different cooling rates were used on the 0.01 wt % solution of rr-P3HT(h) as well as the regio-random P3HT in *p*-xylene and the yields were characterized by SEM, AFM, and UV−vis spectroscopic techniques. In the DSC experiments, the solution placed in the aluminum hermetic pan was heated to 70 °C at the rate of 10 deg/min in the inert atmosphere and then cooled at the rate of 0.5, 1, and 5 deg/min, respectively (Supporting Information). As we found earlier, there was no distinct change in heat flow seen during cooling at different cooling rates, indicating no heat flow from solvent to P3HT for crystallization.

The perforated aluminum hermetic pan was taken out after the DSC experiment and the content dispersed into 5 mL of *p*-xylene by vigorous shaking. This light yellow solution was used for UV−vis and SEM studies. The comparative UV−vis spectra (Figure 2) show the formation of crystal structures of P3HT by closely packed stacking of thioenyl rings at only 0.5 deg/min cooling. The signal at 610 nm has been designated for the absorption of closely packed $\pi-\pi$ stacking structures[1] and a good amount of absorption in this region indicates the crystalline morphology at 0.5 deg/min cooling. No absorption in this region at a higher cooling rate (5 deg/min) and for non-regio-regular P3HT indicates no good crystalline morphology was achieved in these conditions (Figure 2), which corroborates with the finding that nanofiber formation happens at a slower cooling rate.[1,17−19]

To obtain a clear idea about the morphology of the DSC experimentation products, we carried out SEM of these products on silicon substrate. As found in UV−vis experiment, the higher cooling rate and non-regio-regular P3HT formed amorphous structures whereas the slower cooling rates produced fiber type morphology (Figure 3). The SEM image of the product obtained from 1 deg/min cooling rate indicates the fiber formation process was just initiated; this fact is also supported by the UV−vis experimental result. It is therefore a

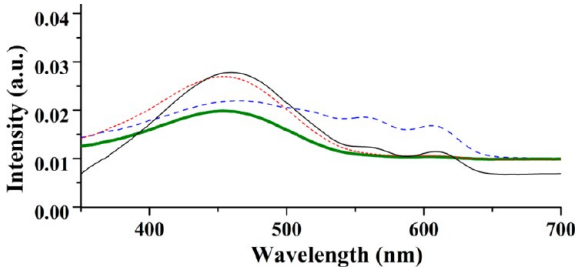

Figure 2. Comparative UV−vis spectra of the DSC experimental yields at different cooling rates. The blue dashed line indicates the heating rate of 10 deg/min and cooling rate of 0.5 deg/min whereas the red dotted line represents the heating rate of 10 deg/min and cooling rate of 5 deg/min of the rr-P3HT. The black thin solid line indicates the heating rate of 10 deg/min and cooling rate of 1 deg/min of the rr-P3HT whereas the green thick solid line represents the same for the non-regio-regular P3HT. The perforated aluminum pans were taken out of the DSC instrument after the experiment and dispersed the content into 5 mL of spectroscopic grade *p*-xylene by vigorous shaking and these light yellow solutions were used for spectroscopic studies.

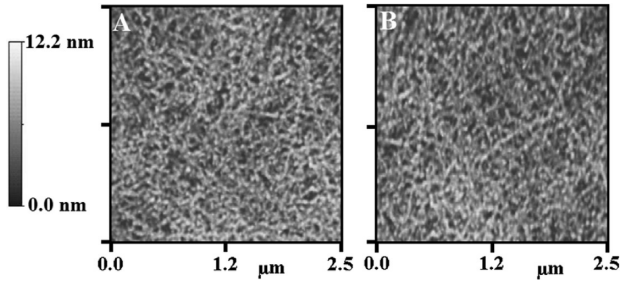

Figure 4. AFM images of the crystallization of rr-P3HT(h) in 0.01 wt % solution at 45 °C (part A) and 35 °C (part B) inside the DSC instrument by isothermal heating for 10 min. Similar thickness and diameter of the crystallite sizes at the different self-assembly temperatures indicate the crystallization temperature does not influence the spherical and rectangular cross section of the crystal size of P3HT in solution.

cooling rate below 1 deg/min that is required for the crystallization by reducing the solubility of rr-P3HT in *p*-xylene. The higher magnification image (Figure 3E) of the self-assembled product at 0.5 deg/min showed that the nanofibers so produced are of 20−25 nm in spherical cross section, i.e., diameter, 3−5 nm in rectangular cross section, i.e., thickness and average length of 300 nm.

For better understanding of the parameters of crystallization of P3HT in solution by the self-assembled product, we then carried out the self-assembly process at different temperatures inside the DSC instrument by isothermal heating with the variable time duration (Supporting Information). The AFM images (Figure 4) suggest that the fiber formations at 45 and 35 °C for 10 min have similar stacking distances along the alkyl side chain and thioenyl $\pi-\pi$ directions and thus the fiber formation temperature does not play any role on the diameter and thickness of the crystallite size of P3HT by self-assembly in solution. However, the duration of the crystallization seems to have a pronounced effect on the length scale of the self-assembled product. The DSC experimental products achieved by isothermal heating at 35 °C for 10 and 1 min duration have the similar diameter and thickness but have different lengths. The SEM images (Figure 5) of the self-assembled product inside the DSC instrument by isothermal heating at 35 °C for 1 min suggest that the average self-assembly length was 200 nm whereas the self-assembly time for 10 min yielded 500−600 nm length.

The length of the nanofibers self-assembled at different temperatures showed negligible effect on the growth temperature; however, the prolonged reaction time (10 min in this case, Figure 5A) allows more lamellar sheets to self-assemble along the fiber axis compared to the lesser reaction time (01 min in this case, Figure 5B). It was found that the length of the

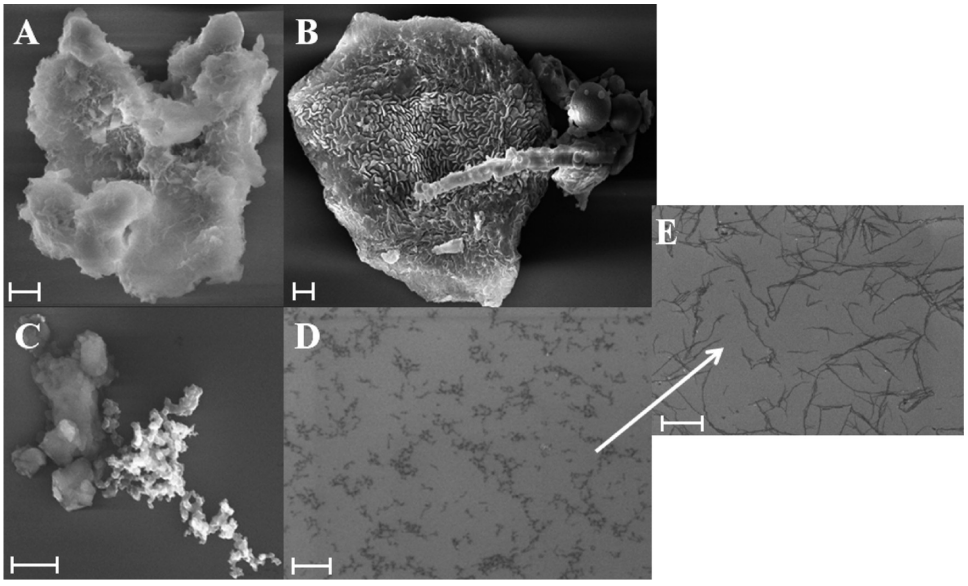

Figure 3. Comparative SEM spectra of 0.01 wt % solution of rr-P3HT(h) and regio-random P3HT dissolved in *p*-xylene at different cooling rates. Part A (scale bar 1 μm) represents the self-assembled product of non-regio-regular P3HT of 0.01 wt % in *p*-xylene achieved by 10 deg/min heating rate and 1 deg/min cooling rate inside the DSC instrument. Parts B, C, and D (scale bar 1 μm each) show the crystallization products of rr-P3HT(h) in *p*-xylene achieved by 10 deg/min heating rate and 5 deg/min, 1 deg/min, and 0.5 deg/min cooling rate. Part E (scale bar 200 nm) stands for the magnified image of the self-assembled product of rr-P3HT(h) by 0.5 deg/min cooling rate.

dx.doi.org/10.1021/jp211408e | *J. Phys. Chem. B* 2012, 116, 7920−7925

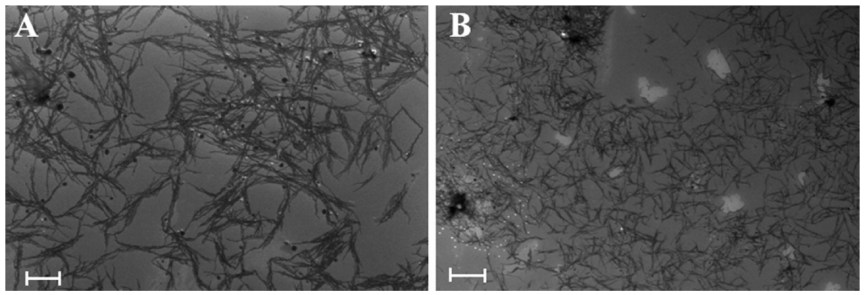

Figure 5. SEM spectra of the self-assembled structure of 0.01 wt % solution of rr-P3HT(h) grown by isothermal heating inside the DSC instrument at 35 °C for 10 min (part A, scale bar 200 nm) and 1 min (part B, scale bar 200 nm), respectively. The higher self-assembly time is the result of the increased crystallite size of rr-P3HT by the orientation of more lamellar sheets along the fiber axis.

self-assembled structure of the 8.2 mg solution of 0.01 wt % of rr-P3HT(h) in *p*-xylene does not grow any longer after the average limiting reaction time of 10 min inside the DSC instrument. This observation leads to the fact that the P3HT crystals achieved either by lowering the temperature of the solvent or by adding nonpolar solvent will produce crystals with similar diameter and thickness and the only difference will be in the length of the fibrous self-assembled product.

To compare the self-assembly process inside the DSC instrument with the actual self-assembly of rr-P3HT, self-assembly of rr-P3HT at 30 deg/h cooling rate on the 0.01 wt % solution of rr-P3HT(h) in *p*-xylene was carried out in a round-bottomed flask with use of the standard procedure.[19] It was found that the average diameter and thickness of the crystallite size of P3HT cooled to 35 and 45 °C are almost similar as seen in the case of the P3HT crystals which were produced inside the DSC instruments. The d_{100} spacings of the P3HT crystal in the small-angle X-ray scattering experiment of the self-assembled products achieved at cooling to 35 and 45 °C are almost similar and corroborates well with the calculated interlamellar spacing of 1.7 nm by the Laue equation (Figure 6).[43,44] The length of the nanofibers self-assembled at different temperatures showed negligible effect on the growth temperature, which resembled the finding of the crystallite length inside the DSC instrument. A 24-h reaction time for 100 mL of rr-P3HT(h) in *p*-xylene resulted in an average crystallite size of 1 μm, whereas the 8-h self-assembly time produced an average 400 nm nanofiber length (Supporting Information). This observation is supported by the fact that the length of the self-assembled structure of 0.01 wt % does not grow any longer after the average limiting reaction time of 24 h.[17−19]

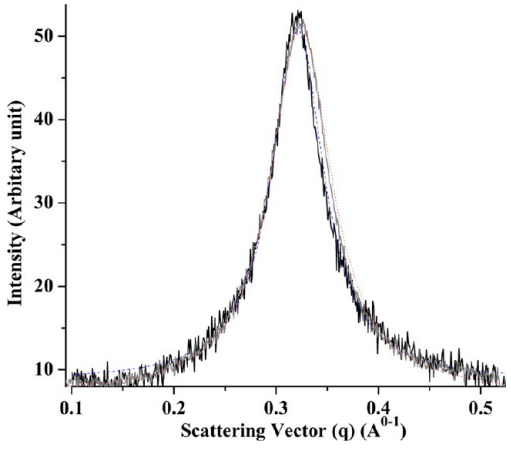

Figure 6. The small-angle X-ray scattering experiment of the self-assembled products of rr-P3HT(h) outside the DSC instrument, achieved at cooling up to 35 °C (gray solid line) and 45 °C (black solid line). The red dotted line and blue dashed lines represent the Lorentzian nonliner curve fitting of the data of 35 and 45 °C, respectively, indicating that the interlamellar spacing is almost similar for the product self-assembled at 45 and 35 °C.

CONCLUSIONS

DSC experiments with different cooling rates failed to detect any shift in the rate of heat loss during the self-assembly process of P3HT in *p*-xylene, the difference in the tangent of heat flow only seen during the change of phase from liquid to solid during the cycle of the second cooling in DSC. By using UV−vis and SEM images of the DSC experimental yields, it was found that a minimum cooling rate below 1 deg/min is required for the crystallization using the self-assembly method by using 0.01 wt % of the higher molecular weight fraction of rr-P3HT solution in *p*-xylene. By using the variable time and temperature of the self-assembled process inside the DSC instrument by isothermal heating, it has been found that the thickness and diameter of the P3HT crystal in *p*-xylene is independent of the growth temperature and duration. The kinetics of the crystallization of P3HT in *p*-xylene across the perpendicular and horizontal direction of the crystal axis is independent of the growth temperature; however, the self-assembly along the crystal axis has been shown to be strongly dependent on the duration of the self-assembly process. The building block of P3HT fibers by the self-assembly process thus has constant stacking distance along the thioenyl ring (diameter) and the alkyl chain (thickness) and is independent of the crystallization parameters or even the way the crystals are formed, such as lowering of the temperature of the solvent or adding nonpolar solvent. The length of the fiber by stacking the building blocks along the fiber axis could be tailored by the duration of the self-assembly process. The non-regio-regular P3HT understandably does not lead to fiber formation in the similar condition due to the difficulties in formation of the highly oriented morphologies.

ASSOCIATED CONTENT

Supporting Information

Figure S1, thermogravimetric analysis of rr-P3HT(h); Figure S2, DSC thermograms of rr-P3HT(h) and regio-random P3HT at a different cooling rates; Figure S3, isochronal cooling of rr-P3HT(h) in *p*-xylene up to the desired temperature followed by isothermal heating; and Figure S4, SEM images of the self-assembled structures achieved outside the DSC instrument at

dx.doi.org/10.1021/jp211408e | J. Phys. Chem. B 2012, 116, 7920−7925

different time intervals of rr-P3HT(h) in *p*-xylene. This material is available free of charge via the Internet at http://pubs.acs.org.

AUTHOR INFORMATION

Corresponding Author

*E-mail: debmalya_roy@yahoo.com. Phone: 0512-2451759 to 78. Fax: 0512-2450404 & 2404774.

Notes

The authors declare no competing financial interest.

ACKNOWLEDGMENTS

The authors gratefully acknowledge the help from Prof. Ashutosh Sharma and Mr. Alok Srivastava, DST Unit of Nanoscience, IIT, Kanpur for the SEM and SAXS experiments. We thank Director, National Physical Laboratory (NPL), New Delhi for permitting us to record the AFM images. We are thankful to Dr. R. Ramani, polymer science division, DMSRDE for thermal analysis experiments. Babita thanks the Defence Research and Development Organization (DRDO), New Delhi for a senior research fellowship. The authors thank Prof. Vikram Kumar, Department of Physics, IIT, Delhi, Prof N. Sathyamurthy, Indian Institute of Science Education & Research (IISER) Mohali, Chandigarh and Prof. A. J. Pal, Solid State Physics, Indian Association for the Cultivation of Science (IACS), Kolkata for helpful discussions and suggestions. The authors also acknowledge the expert advices of Prof. Richard D. McCullough, Carnegie Mellon University, Pittsburgh, USA. The authors are grateful to the Director, DMSRDE, Kanpur for help and support and for permitting us to use our experimental findings.

REFERENCES

(1) Leclère, P.; Surin, M.; Brocorens, P.; Cavallini, M.; Biscarini, F.; Lazzaroni, R. *Mater. Sci. Eng.* **2006**, *55*, 1.

(2) O'Neil, K. D.; Shaw, B.; Semenikhin, O. A. *J. Phys. Chem. B* **2007**, *111*, 9253.

(3) Rahman, A.; Sanyal, M. K.; Gangopadhyay, R.; De, A. *Chem. Phys. Lett.* **2007**, *447*, 268.

(4) Stutzmann, N.; Friend, R. H.; Sirringhaus, H. *Science* **2003**, *299*, 1881.

(5) Pal, S.; Nandi, A. K. *Polymer* **2005**, *46*, 8321.

(6) Moreno, M.; Casalegno, M.; Raos, G.; Meille, S. V.; Po, R. *J. Phys. Chem. B* **2010**, *114*, 1591.

(7) Masubuchi, S.; Kazama, S. *Synth. Met.* **1995**, *74*, 151.

(8) Babel, A.; Jenekhe, S. A. *J. Phys. Chem. B* **2003**, *107*, 1749.

(9) Rughooputh, S. D. D. V.; Hotta, S.; Heeger, A. J.; Wudl, F. *J. Polym. Sci., Polym. Phys.* **1987**, *25*, 1071.

(10) O'Brien, G. A.; Quinn, A. J.; Iacopino, D.; Pauget, N.; Redmond, G. *J. Mater. Chem.* **2006**, *16*, 3237.

(11) Liu, H.; Reccius, C. H.; Craighead, H. G. *Appl. Phys. Lett.* **2005**, *87*, 253106.

(12) Zhang, X.; MacDiarmid, A. G.; Manohar, S. K. *Chem. Commun.* **2005**, 5328.

(13) Bjørnholm, T.; Hassenkam, T.; Greve, D. R.; McCullough, R. D.; Jayaraman, M.; Savoy, S. M.; Jones, C. E.; McDevitt, J. T. *Adv. Mater.* **1999**, *11*, 1218.

(14) Maynor, B. W.; Filocamo, S. F.; Grinstaff, M. W.; Liu, J. *J. Am. Chem. Soc.* **2002**, *124*, 522.

(15) Liu, J.; Sheina, E.; Kowalewski, T.; McCullough, R. D. *Angew. Chem.* **2002**, *114*, 339.

(16) Samitsu, S.; Iida, T.; Fujimori, M.; Heike, S.; Hashizume, T.; Shimomura, T.; Ito, K. *Synth. Met.* **2005**, *152*, 497.

(17) Zhang, R.; Li, B.; Iovu, M. C.; Jeffries-EL, M.; Sauvé, G.; Cooper, J.; Jia, S.; Tristram-Nagle, S.; Smilgies, D. M.; Lambeth, D. N.; McCllough, R. D.; Kowalewski, T. *J. Am. Chem. Soc.* **2006**, *128*, 3480.

(18) Samitsu, S.; Shimomura, T.; Ito, K. *Thin Solid Films* **2008**, *516*, 2478.

(19) Yang, C.; Orfino, F. P.; Holdcroft, S. *Macromolecules* **1996**, *29*, 6510.

(20) Xu, W.; Li, L.; Tang, H.; Li, H.; Zhao, X.; Yang, X. *J. Phys. Chem. B* **2011**, *115*, 6412.

(21) Zhang, R.; Li, B.; Iovu, M. C.; Jeffries, M.; Sauve, G.; Cooper, J.; Jia, S.; Nagle, S. T.; Smilgies, D. M.; Lambeth, D. N.; McCullough, R. D.; Kowalewski, T. *J. Am. Chem. Soc.* **2006**, *128*, 3480.

(22) Berson, S.; Bettignies, R. D.; Bailly, S.; Guillerez, S. *Adv. Funct. Mater.* **2007**, *17*, 1377.

(23) Zhao, Y.; Shao, S.; Xie, Z.; Geng, Y.; Wang, L. *J. Phys. Chem. C* **2009**, *113*, 17235.

(24) Sun, S.; Salim, T.; Wong, L. H.; Foo, Y. L; Boey, F.; Lam, Y. M. *J. Mater. Chem.* **2011**, *21*, 377.

(25) Kroon, R.; Lenes, M.; Hummelen, J. C.; Blom, P. W. M.; Boer, B. D. *Polym. Rev.* **2008**, *48*, 531.

(26) Krebs, F. C.; Spanggaard, H. *Chem. Mater.* **2005**, *17*, 5235.

(27) Halls, J.; Comil, J.; Santos, D. A.; Sibey, R.; Hwang, D. H.; Holmes, A. B.; Bredas, L. J.; Friend, R. H. *Phys. Rev. B* **1999**, *60*, 5721.

(28) Roy, D.; Shastri, B.; Imamuddin, M.; Mukhopadhyay, K.; Rao, K. U. B. In *Intelligent Nanomaterials*; Tiwari, A., Mishra, A. K., Kobayashi, H., Turner, A. P. F., Eds.; Wiley-Scrivener: Salem, MA, 2011; pp 425−466.

(29) Roy, D.; Shastri, B.; Imamuddin, M.; Mukhopadhyay, K.; Rao, K. U. B. *Renewable Energy* **2011**, *36*, 1014.

(30) Ewbank, P. C.; Laird, D.; McCullough, R. D. In *Organic Photovoltaics*; Brabec, C., Dyakonov, V., Scherf, U., Eds.; Wiley-VCH Verlag GmbH: Weinheim, Germany, 2009; pp 3−20.

(31) Merlo, J. A.; Frisbie, C. D. *J. Phys. Chem. B* **2004**, *108*, 19169.

(32) Liu, J.; Sheina, E.; Kowalewski, T.; McCullough, R. D. *Angew. Chem., Int. Ed.* **2002**, *41*, 329.

(33) Li, L. G.; Lu, G. H.; Yang, X. N. *J. Mater. Chem.* **2008**, *18*, 1984.

(34) Kiriy, N.; Jähne, E.; Adler, H. J.; Schneider, M.; Kiriy, A.; Gorodyska, G.; Minko, S.; Jehnichen, D.; Simon, P.; Fokin, A. A.; Stamm, M. *Nano Lett.* **2003**, *3*, 707.

(35) Malik, S.; Jana, T.; Nandi, A. K. *Macromolecules* **2001**, *34*, 275.

(36) Kim, D. H.; Park, Y. D.; Jang, Y.; Kim, S.; Cho, K. *Macromol. Rapid Commun.* **2005**, *26*, 834.

(37) Park, B.; Aiyar, A.; Park, M. S.; Srinivasarao, M.; Reichmanis, E. *J. Phys. Chem. C* **2011**, *115*, 11719.

(38) Brinkmann, M. *J. Polym. Sci., Part B: Polym. Phys.* **2011**, *49*, 1218.

(39) Tompa, A. S.; Bryant, W. F. *Thermochim. Acta* **2001**, *367*, 433.

(40) Torrent, M.; Boer, D.; Durkut, M.; Hadley, P.; Schenning, A. P. H. J. *Nanotechnology* **2004**, *15*, 265.

(41) Zhao, Y.; Yuan, G.; Roche, P.; Leclerc, M. *Polymer* **1995**, *36*, 2211.

(42) Samitsu, S.; Shimomura, T.; Heike, S.; Hashizume, T.; Ito, K. *Macromolecules* **2008**, *41*, 8000.

(43) Wu, P. T.; Xin, H.; Kim, F. S.; Ren, G.; Jenekhe, S. A. *Macromolecules* **2009**, *42*, 8817.

(44) Dai, C. A.; Yen, W. C.; Lee, Y. H.; Ho, C. C.; Su, W. F. *J. Am. Chem. Soc.* **2007**, *129*, 11036.